Published in final edited form as:
J Magn Reson Imaging. 2013 November ; 38(5): . doi:10.1002/jmri.24082.

BOLD fMRI in Infants under Sedation: Comparing the Impact of Pentobarbital and Propofol on Auditory and Language Activation

Mark W. DiFrancesco, Ph.D.[1,*], **Sara A. Robertson**[1], **Prasanna Karunanayaka, Ph.D.**[2], and **Scott K. Holland, Ph.D.**[1]

[1]Cincinnati Children's Hospital Medical Center, Pediatric Neuroimaging Research Consortium, Cincinnati, OH 45229, USA

[2]Department of Radiology (Center for NMR Research), The Pennsylvania State University College of Medicine, The Milton S. Hershey Medical Center, Hershey, PA 17033, USA

Abstract

Purpose—To elucidate differences in the disruption of language network function, as measured by BOLD fMRI, attributable to two common sedative agents administered to infants under clinical imaging protocols.

Materials and Methods—The sedatives pentobarbital (Nembutal) and Propofol, administered clinically to infants at one year of age, were compared with respect to BOLD activation profiles in response to passive story-listening stimulation. An intermittent event-related imaging protocol was utilized with which the temporal evolution of language processing resulting from this stimulation was explored.

Results—Propofol and Nembutal were found to have distinct and complementary responses to story-listening. Propofol exhibited more activation in higher processing networks with increasing response toward the end of narrative stimulus. Nembutal, in contrast, had much more robust activation of primary and secondary sensory cortices but a decreasing response over time in fronto-parietal default-mode regions. This may suggest a breakdown of top-down feedback for Propofol vs. the lack of bottom-up feed-forward processing for Nembutal.

Conclusion—Two popular sedative agents for use in children for clinical fMRI were found to induce distinct alteration of activation patterns from a language stimulus. This has ramifications for clinical fMRI of sedated infants and encourages further study to build a framework for more confident interpretation.

Keywords

anesthesia; sedation; fMRI; language; infants; Propofol; Pentobarbital

Introduction

Functional magnetic resonance imaging (fMRI), based on blood oxygenation level-dependent (BOLD) contrast, has been developing over the last two decades(1) as an important tool for brain research. Key to its application and interpretation is evidence that

[*]Corresponding Author: Mark W. DiFrancesco, Ph.D., Pediatric Neuroimaging Research Consortium, Cincinnati Children's Hospital Medical Center, 3333 Burnet Ave, ML 5033, Cincinnati, OH 45229-3039, USA. Phone: (513) 636-0436, Fax: (513) 636-3754, Mark.DiFrancesco@cchmc.org.

local changes in blood oxygenation in the brain are coupled to local changes in neuronal activity through a characteristic hemodynamic response mechanism(2). An extensive literature describes numerous studies employing BOLD fMRI that have revealed the impact of disease or other challenges on regional brain response to cognitive and sensory stimulation(3–5).

More recently, the utility of fMRI has been extended to clinical use in radiology where it is applied most commonly to map eloquent cortex for presurgical planning(6,7). Due to their importance for quality of life, functional domains such as motor and language ability are now mapped using fMRI prior to surgery in order to identify brain regions that would result in morbidity if damaged. An extensive history of functional imaging research in these domains has allowed the choice of effective stimuli to evoke the intended brain activity and the confident radiological interpretation of resulting activation maps.

Functional MRI, being a noninvasive procedure, can be applied in children, even serially, to study the developing brain. Such studies, however, become increasingly difficult to administer as younger children are considered for inclusion. In fact, research cohorts are nearly always confined to ages five and older because younger children require sedation in order to tolerate the procedure and to remain motionless. Pharmacological sedation of children is not ethical if undertaken solely for research, so with the exception of some studies completed under natural sleep protocols(8), fMRI investigations of development covering the critical years from infancy to preschool age are lacking. Clinically sedation is routinely administered to the youngest patients referred for imaging assessment by radiology (9,10). If fMRI is to be performed on these patients, passive stimuli are presented to elicit activity in targeted brain networks.

Sedation complicates administration and interpretation of fMRI in the clinical setting. The mechanisms by which altered states of consciousness result from sedation and anesthesia are not well understood. Theories include a loss of information integration in higher processing areas(11) or a loss of cognitive “binding” between lower level sensory cortices and higher associative and integrative regions(12). Several recent investigations of the effect of sedation on activation and connectivity patterns in cognitive and default-mode networks(13) suggest such a disintegration of meaningful information transfer(14). How network disruptions precipitated by sedation will manifest as modifications of expected activation patterns for given fMRI stimuli is not clear. This is further complicated by evidence that sedative agents have the potential to alter both neuronal response and the hemodynamic coupling on which the BOLD effect relies(15). Such modifications of the BOLD response are likely to depend on the method of sedation, including the choice of drug agent and dosing. Thus, confident interpretation of fMRI for the critical years of birth to preschool age requires an understanding of the expected activation signatures in the context of the applied sedation protocol.

The work presented here compares two popular MRI sedation protocols, based on Propofol and Nembutal, in regards to their impact on brain activation in infants subjected to stimuli meant to invoke narrative comprehension. Data were collected as part of the control arm of a study that compared bilaterally hearing-impaired infants in a narrow age range to age-matched normal-hearing controls with respect to BOLD response to story listening(16). The goal of the analysis presented is to begin to elucidate the influence of these sedation protocols on the BOLD effect used for fMRI mapping of brain activity. The imaging data were collected during modest extensions of clinical radiological exams conducted on infants under sedation. Due to the clinical setting, strict experimental control over all sedation parameters was not possible. Thus, this study addresses differences in clinical sedation protocols in their entirety, but does not determine differences specific to the sedative agents.

Story listening offers potential for rich insight as it elicits language processing at multiple levels with temporal hierarchy including sound, word, and sentence processing, culminating with comprehension of multiple sentences as a cohesive narrative(17,18). An intermittent event-related imaging protocol(19) used in this study permits auditory stimulus presentation without interfering scanner noise and a degree of temporal parsing of response. For normal-hearing subjects, response to story listening was compared between sedation groups in progressive time windows with respect to activation in expected language areas and canonical default-mode regions.

Materials and Methods

Subjects

Twenty infants in the age range of 8–17 months participated in a clinically indicated brain MRI study under sedation (15 females, 5 males, mean age = 12.5 months, SD = 2.9 months). Subjects were recruited from the clinical MRI schedule and met inclusion criteria of: gestational age of at least 36 weeks, normal otoacoustic emissions hearing, and referral for reasons not related to hearing; see Table 1 for a complete list of referrals. The brains of all subjects were considered to be grossly normal, based on review of scans by pediatric neuroradiologists.

The study was conducted with approval from a pertinent Institutional Review Board. Written informed consent was attained from parents or guardians of all subjects before their participation in this research study.

Sedation

Sedation protocols for clinical MRI were comprised of either pentobarbital (oral Nembutal, n = 11, 7 females, 4 males, average age = 12.5 months, SD = 3.1 months) with a dosage of 5 mg/kg, or IV Propofol (n = 9, 8 females, 1 male, average age = 12.4 months, SD = 2.9 months) with a dosage of 200–300 mcg/kg/min and 8% Sevofluorane induction. These protocols were applied to each subject with occasional variations deemed necessary by the attending anesthesiologist to maintain clinical sedation. It is reasonable to expect that residual effects of Sevofluorane induction, administered an average of one hour prior to fMRI acquisition, were negligible given adequate tidal volume to clear the lungs. Details of each subject’s dosage are included in Table 1.

fMRI Paradigm

A paradigm targeting narrative comprehension was employed during functional imaging while each subject was under sedation. Stimulation occurred in epochs consisting of a period of passive listening to two sentences of a story, a period of broad-band noise tones and a period of silence. Each subject heard story sentences recorded by the same adult female. One of two schemes of stimulus ordering was applied randomly among the subjects: stories/silence/tones or the reverse. Stimuli were administered in the context of a clustered imaging technique, Hemodynamics Unrelated to Sounds from Hardware (HUSH)(19), which alternates imaging periods with non-imaging (quiet) periods during which auditory stimulation can be heard without interference from gradient noise. This study specifically used a 5-second non-imaging period for stimulus presentation followed by a 6-second imaging period capturing the hemodynamic response to the preceding stimuli. Auditory stimuli were administered through calibrated MR compatible headphones and set to 85dB hearing level. This threshold was selected as a comfortable hearing level that would be clearly audible by infants with normal hearing as measured by otoacoustic emission administered immediately prior to the MRI.

fMRI Image Acquisition

Functional imaging acquisition followed immediately after each subject's prescribed clinical protocol on a 3 Tesla Siemens Trio scanner in the clinical Radiology Department at our institution. During each of the 6-second imaging periods described above, three T2*-weighted gradient echo EPI images, designated volume 1, 2, and 3, were acquired, each using: TR=2000 ms, flip angle=77.6° (Ernst angle), TE=38 ms, 64 × 64 matrix, 256 mm × 256 mm FOV, 25 slices with 5 mm thickness. Twenty epochs comprised of the three stimulus types outlined above were acquired for a total scan time of 11 minutes. A high-resolution 3D T1-weighted, MPRAGE (20) image was acquired for each subject using with a spatial resolution of 1 × 1 × 1 mm, TR/TE/TI = 2000/2.93/1000 ms, FOV = 21.9 × 21.9 cm, matrix = 256 × 205, and scan time = 3 minutes 50 seconds. The T1-weighted images served as anatomical reference after co-registration with the fMRI images.

Data Pre-processing

Image reconstruction was executed using in-house software, which was developed in IDL (Interactive Data Language, ITT Visual Information Solutions, Boulder, CO). This software allowed the use of a multi-echo phase reference scan through which functional images were corrected for geometrical distortion(21). Reconstructed images were spatially pre-processed using Statistical Parametric Mapping software (SPM8, www.fil.ion.ucl.ac.uk/spm). For the HUSH protocol, image series for volumes 1, 2, and 3 were treated separately, including initially aligning the first images of each series to each other followed by realignment of the images within each series to the first image of the series. After co-registration of the anatomic reference image to the resulting mean functional image, normalization to a common space was performed in SPM8 concurrently with tissue class segmentation based on gray matter, white matter, and cerebro-spinal fluid templates suited specifically for infant brains(22). Spatial processing was completed by smoothing with an 8 mm FWHM Gaussian. The intermittent imaging characteristic of the HUSH protocol means that volumes 1, 2, and 3 are at different stages of T1 relaxation and consequently vary in mean intensity and signal variance. Thus, baseline intensity was removed from analysis by using the logarithm of the functional signal.

Data Analysis

Individual Subjects—Statistical parametric maps (SPMs) for individual subjects were obtained by pairwise contrast of BOLD signal between stimulus conditions within each epoch. Our analysis exploits the factorial nature of the study design, in which there are two within-subject factors and one between-subject factor. The within-subject factors are time (volumes 1, 2 and 3) and condition (stories, tones, and silence). The between-subject factor is the sedative drug. Our particular interest here was the two-way interaction between drug and condition; in other words, a modulation of language-related activations by the different anesthetics. We were also interested in the three-way interaction; namely the effect of drug on the interaction between time and condition. This interaction reflects time-dependent hemodynamic responses elicited by language stimuli. Three contrasts were considered: stories vs. silence, stories vs. tones, and tones vs. silence. The tones vs. silence contrast was meant to represent auditory response while the stories vs. tones contrast was designed to reflect higher language function excluding sensory processing. The study results presented here focus primarily on the stories vs. silence contrast as this represents the full range of auditory and language processing for narrative comprehension and tends to give the strongest contrast.

Exploration of time-resolved hemodynamic response was motivated by the temporal characteristics of the narrative comprehension task applied in this study. Stimuli that induce brain activity throughout the 5-second period prior to image acquisition in the HUSH

protocol will have a peak hemodynamic response (assuming a canonical transfer function peaking at about 5 seconds) at about the midway point of the volume 2 acquisition. Brain activity induced only at the end of the stimulus period, however, doesn't peak in BOLD response until sometime during volume 3, while a peak in volume 1 would occur if stimuli were restricted to the beginning of the stimulus period. These characteristic BOLD responses, illustrated in Figure 1, are presented to demonstrate the potential for observed responses sculpted by the accumulated effects, both positive and negative, of evolving language processing evoked during the stimulus period. The factorial design of our analysis allows some level of dissection of the temporal response of the resulting BOLD signal to the narrative segments.

Group Composites—Parameter contrast maps of individual subjects were taken to the second level for random effects analysis(23) testing for mean contrast for each sedation group and for the difference in contrast between sedation groups, generating composite SPMs of the t-statistic in each case.

Region of Interest Analysis—The relatively low numbers of subjects in each sedation group motivated a region of interest (ROI) approach to supplement the voxel-wise assessment outlined above. A narrative comprehension task has the expectation to activate or deactivate specific anatomically-defined brain regions(24,25), including semantic processing regions summarized by Binder et al.(26). For this analysis, 12 regions were considered, each separated into right and left hemisphere portions (Figure 2). Masks for these ROI were extracted from the Wake Forest University Pick-Atlas Toolbox(27) incorporated in SPM8.

ROI masks were employed in two ways in an effort to improve sensitivity. First, the masks were used to define limited regions over which to apply a small volume correction (SVC) for multiple comparisons in lieu of considering the whole brain volume. Second, ROI masks were applied to each of the contrast maps for individual subjects to obtain an aggregate measure of regional response. Our analysis defined aggregate response as the mean of all voxel contrast values within each corresponding mask..

The mean aggregate measures for the Nembutal and Propofol groups were determined for each ROI. In addition, the differences in mean ROI aggregate measures between the Nembutal and Propofol groups were calculated. A bootstrap approach was employed, generating 10,000 resamples, with replacement, for the Nembutal and Propofol groups separately calculating group means and the difference between group means for each resample. The resulting distributions of means or differences were examined to determine mean group means and the probability (p-value) of falsely rejecting the null hypothesis of zero mean group mean. Results with p-values < 0.05 are reported as statistically significant.

Results

Group Composites

Group composite maps, showing the mean response of all 3 image volumes, for the stories vs. silence contrast in Nembutal and Propofol groups are shown in Figure 3, A and B respectively. Activation (stories > silence), using a threshold of $p < 0.005$, uncorrected for multiple comparisons, is evident in auditory cortex and surrounding regions of Brodmann Area (BA) 22 under Nembutal while these areas fail to activate under the influence of Propofol. Deactivation (silence > stories) was apparent in the thalami for both groups. The difference map in Figure 3C, at the same threshold, shows a cluster in left auditory cortex plus a small region of right anterior BA22 stronger in Nembutal compared to Propofol. Refer to Table 2 for a corresponding list of significant clusters at the $p < 0.05$ level, family-

wise error (FWE) corrected. Note that, for simplicity, all tables report corrected p-values using SVC for clusters that fall within one of the specified ROI. Any clusters not covered by an ROI yet significant after correction over the whole brain, are also reported and marked with an asterisk.

For the contrast reflecting the interaction between the stories vs. silence contrast and time (image volume), the resulting group SPMs are shown in Figure 4 for the Nembutal group (4A), the Propofol group (4B) and for Nembutal > Propofol (4C) at the threshold of $p < 0.005$ uncorrected. The sign of the parameters in these maps reflects the slope of the hemodynamic response for the stories vs. silence contrast, between volume 1 and volume 3. The group under Nembutal had clusters of exclusively negative interaction (stories vs. silence response contrast decreasing from volume 1 to volume 3) in multiple regions including several frontal and temporal language ROI, thalamus, brainstem, and inferior occipital lobe. Subjects sedated under Propofol shared the negative interaction in thalamus observed under Nembutal, but lacked clusters of negative slope in other regions using the chosen threshold. On the other hand, the Propofol group had a few small clusters of positive interaction in the parahippocampal gyrus, cingulate, and dorsal prefrontal areas. These marked differences in slope of response between drug groups are reflected in the difference map of Figure 4C.

Other contrasts between conditions, including stories vs. tones and tones vs. silence were also considered but resulted in only weak mean responses across the three volumes. Interaction of stories vs. tones with image volume was significantly negative in clusters of medial frontal and inferior parietal ROI as well as cerebellum under Nembutal while no significant clusters were found under Propofol. Interaction for tones vs. silence was significant only for right thalamus under Nembutal with negative slope.

Region of Interest Analysis using Aggregate Contrast

Activation as measured by aggregate contrast differed between Nembutal and Propofol subject groups for a variety of canonical language and default-mode ROIs shown in Figure 2. Table 4 lists the ROI with statistically significant activation for the Nembutal and Propofol groups using the aggregate measure of mean response for the three image volumes. The stories vs. silence contrast produced activation for the Nembutal group restricted to primary and secondary auditory ROIs. Activation for the Propofol group also included primary auditory cortex but extended further to higher order language ROIs in the inferior parietal lobe, left and right. The thalamus deactivated for both drug groups. The activation pattern for Propofol persisted for the stories vs. tones contrast while the Nembutal group failed to activate any ROI for that contrast. The tones vs. silence contrast resulted in deactivation of medial frontal regions only for Nembutal. At the statistical threshold chosen, no significant differences between drug groups were found for any contrast for any ROI.

ROI aggregate measures for the interaction of condition and time (image volume), representing the slope of the hemodynamic response between volume 1 and volume 3, had significant composite values for the Nembutal and Propofol groups as shown in Table 5. Striking are the complementary outcomes for the two drug groups for stories vs. silence: Under Nembutal, the slope of the hemodynamic response is exclusively negative in a variety of frontal, parietal, and temporal ROIs, while under Propofol, the response slopes are positive in nearly all responsive ROIs. The exceptions are the thalamic ROI for which both drugs show a negative slope. ROIs with significant differences between drug groups are listed in Table 6. As the group composites from Table 5 suggested, many ROIs were found to have a significantly greater slope for the Propofol group compared to the Nembutal group.

Thalamic, prefrontal, and temporal regions had persistent negative interaction effects for the stories vs. tones contrast under Nembutal while Propofol failed to show significant interaction for this contrast. Tones vs. silence, remarkably, repeated much of the positive and negative interaction effects observed for Propofol under stories vs. silence while the Nembutal group only interacted negatively in the dorsal prefrontal ROI.

Discussion

Two sedation protocols in common use today for pediatric clinical MRI have been compared regarding BOLD activation resulting from the exercise of narrative comprehension in infants. Listening to sentences of a story elicits a hierarchy of auditory and language processing separable in time(17,18,28). An intermittent, event-related, image acquisition protocol(19) permits presentation of stories in the absence of scanner noise, followed by three consecutive image volumes measuring BOLD signal response at different delay times. Using this approach, this study compared sedation protocols according to stage of language processing by measuring both the mean and time-dependent response during image acquisition.

The two drugs considered in this study, Nembutal and Propofol, were each administered by an anesthesiologist according to a clinical protocol established for MRI in our Radiology department, to diminish consciousness in infants undergoing an MRI exam. The neurofunctional implications of the loss of consciousness are the subject of ongoing theoretical treatment and experimental research. Consciousness requires brain networks to have a rich palette of available states. Information emerges by selection of specific states via functional integration of specialized network processing modules. This theme is expressed by a number of current theoretical frameworks including information integration theory(11), the global workspace theory(29), and the concept of cognitive binding(12,14). Loss of consciousness may result from severe restriction of available states and/or disruption of network integration. In this context, some networks arise as having special importance for maintaining consciousness. The integrity of thalamocortical circuits appears to be essential(11), though it is not clear whether anesthetic breakdown of this circuitry is always due to effects on the thalamus directly or to the lack of feedback to the thalamus from deactivated cortical regions. Maintenance of a fronto-parietal axis of connections also appears to be necessary for conscious processing(11,30). This network shares elements with the default-mode network and connects regions of the medial frontal lobe with the sensory-associative regions situated more posteriorly in the parietal region and the PCC.

Experiments have shown that sedation diminishes BOLD activation invoked by passive tasks during fMRI, especially for higher-order cognitive function(31). Activation in primary sensory regions tends to be maintained in comparison, but with intensity that decreases with dosage of sedative agent(31). Much of the experimental work on sedation to date has focused on measuring changes in the functional connectivity of brain networks based on interregional correlation of spontaneous BOLD signal fluctuations recorded during rest(32). On a theoretical basis, this connectivity relates to the integration of processing in separate functional units necessary for consciousness. It has been shown that functional connectivity, particularly between low-level sensory/associative cortices and regions responsible for high-level cognitive processing, is disrupted by sedation(33,34).

A subset of experimental investigations of the effects of sedation focuses on the language domain. Again, it has been found that, under auditory stimulation, activation in higher order association cortices disappears even under light doses of Propofol, while primary and secondary auditory regions continue to activate even in deep sedation, though to an extent diminishing with dose(31). Response to speech perception, specifically, has been observed

in bilateral superior and middle temporal lobe even under deep Propofol sedation while neural correlates of speech comprehension in posterior temporal regions fail to activate even at mild sedation levels(35). Despite the loss of activation invoked by auditory and language stimuli under sedation, functional connectivity within higher-order regions responsible for multimodal integration as well as semantic and memory processing has been found to persist(36), while binding of these regions to low-level sensory cortices breaks down (37). Recent work, employing an effective connectivity model, suggests more specifically that Propofol sedation disrupts backward connections from frontal to parietal processing nodes (38).

The primary focus of the remaining discussion will be on the contrast between the stimulus conditions of story listening and silence as this includes all levels of auditory/language processing involved in narrative comprehension. The other contrasts, including stories vs. tones and tones vs. silence, were intended to isolate language and auditory processing, respectively. Where applicable, these contrasts will also be considered for discussion, though they generally provided less robust activation compared to the stories vs. silence contrast.

Mean voxel-wise BOLD response over the three image volumes resembled the typical findings of other investigators (31,39). Activation was robust under Nembutal for stories vs. silence contrast in auditory cortex and surrounding superior temporal regions, while the thalami deactivated. Voxel-wise response was weakened under Propofol to the point of no significant activation or deactivation.

Aggregate ROI measures, on the other hand, reveal a salient difference in brain activity between the Propofol and Nembutal sedation protocols (Table 4). While the stories vs. silence contrast commonly activates primary and secondary auditory cortices with deactivation of the thalami for both sedation protocols, Propofol sedation alone allows significant engagement of bilateral ROIs comprising the inferior parietal lobule (IPL). This outcome for Propofol persisted under the stories vs. tones contrast designed to isolate language processing. Thus, while Nembutal response is confined to low-level auditory/ language modules, Propofol additionally engages higher-level integrative language areas, such as the IPL, necessary for comprehension.

The interaction of condition and time, represented by image volume number, characterized the linear component of the time-dependent response (response slope) during the 6-second imaging window following stimuli. Widespread significant interactions were found principally for the Nembutal protocol by voxel-wise analysis (Figure 4 and Table 3). It is notable that across all ROI and all condition contrasts with significant interaction, response under Nembutal was suppressed at late times (volume 3) compared to early times (volume 1).

Aggregate measures of the slope of response were markedly different between the Nembutal and Propofol sedation protocols. Exclusively negative response slopes under the Nembutal protocol in many of the language and default mode ROI, were countered by positive slopes, reflecting enhancement of response at late times (volume 3) compared to early times (volume 1), under the Propofol protocol. Though the temporal responses for Nembutal and Propofol were largely complementary, the thalami responded similarly with a negative slope for both sedation groups.

Typically, an event-related design will apply very brief stimuli compared to the duration of the canonical hemodynamic response function (HRF). An extended five-second period of story listening stimuli opens the possibility that different stages of language processing, culminating in narrative comprehension, can be underway at different times. Thus,

distinctions in response slope observed in this study may reflect changing levels of activation or deactivation evoked at different times in response to the narrative stimuli.

Interpretation of this study's outcomes is aided by adaptation of an effective connectivity model by Boly et al. (38) that includes a thalamic, a frontal, and a parietal node, each connected reciprocally. Under Propofol sedation, this model is altered by increased excitability of the thalamic node and a breakdown of backward connectivity from the frontal to parietal node. In the context of narrative stimulation, we propose augmenting this model by the addition of auditory input to the thalamic node plus an auditory sensory (temporal) node connected to the thalamic node and the two higher nodes. Subsequent discussion will allow that the frontal and parietal nodes of this model can subserve either high-order integrative language processing or default mode processing.

Aggregate ROI measures show mean activation of high-level parietal regions under Propofol while only primary auditory and surrounding temporal regions activate under Nembutal. Using the augmented model described above, this suggests preservation of feed-forward connections from auditory to parietal nodes for Propofol but a breakdown of that connection for Nembutal. The thalamus is commonly deactivated under both protocols, perhaps reflecting interruption of the hyperexcitability of the thalamic node due to processing of external input. Results of this study and others (31,39) make it reasonable to assume that both sedation protocols maintain connectivity between thalamic and auditory nodes and, as reported by Boly et al. (38), that reciprocal connections from the thalamic and higher-order nodes remain intact. Linear trend of response to stories vs. silence, using aggregate ROI measures, was dramatically different between the Nembutal and Propofol protocols. In a variety of fronto-parietal areas, response trended downward at late times under Nembutal while it trended upward under Propofol. The negative trend was also observed in auditory temporal regions under Nembutal. These trends and their distinctions might be attributed to evolving, increasingly complex, language processing in the course of listening to sentences of a story following a model for nodal connectivity that is altered differently by the two sedation protocols. As the auditory narrative stream continues during each stimulus period, feed-forward connections maintained under Propofol increasingly allow engagement of parietal and then frontal regions for content integration. Failure of backward connectivity from frontal to parietal nodes, however, might prevent top-down exchange from higher to lower processing nodes. Under Nembutal, conversely, it appears that information is not delivered to the fronto-parietal nodes from auditory regions. Instead, the effects of auditory input are communicated to those higher nodes solely through the thalamus. With no processed input from the auditory node, ongoing default-mode processing in the fronto-parietal nodes is increasingly disrupted by more and more complex input relayed through the thalamus. This results in decreasing response in fronto-parietal nodes as time progresses through the presentation of story sentences. In the same way, a hyperactive thalamus has a mean deactivation in response to story-listening with a negative trend of response over time, in common to both Nembutal and Propofol sedation.

In summary, contrasting linear trends in ROI aggregate measures for Nembutal and Propofol protocols suggest differences in brain activity developed toward the end of the stimulus period after the subject had listened to nearly the entirety of both sentences. The IPL and PCC regions exemplify this behavior. These regions are understood to be crucial for narrative comprehension (18,24,25,40), integrating past knowledge and experience. Notably, these same regions are part of the default mode network(13), which is suppressed during attention to input. Late response to stories vs. silence is differentiated between sedation groups with the Nembutal group suppressing activity while the Propofol group enhances response in these regions. This suggests that while the Propofol group is attempting to

integrate internally or externally generated elements of experience, the Nembutal group is engaged in suppression of that process in favor of attention to external auditory stimuli.

Interpretation of the dichotomy of response patterns between sedation protocols remains speculative as other factors may play a role and key information is lacking. Sedative agents can impact cerebral blood flow in different ways by vasoactivity (15), thus altering the HRF on which the BOLD effect relies. It is unclear to what extent differences between Nembutal and Propofol regarding blood flow might explain the observed differences in BOLD temporal response between the two protocols. A full explanation based merely on shape of the HRF is dispelled to some degree by the fact that the thalamus behaves identically, for both average response and slope of response, for the two sedation protocols. As noted above, changes in activation due to sedation are directly related to the depth of sedation. The data discussed here were, by necessity, acquired in a clinical setting restricted to standard protocols. Even though Propofol and Nembutal dosing by weight was consistent among the subjects, no measurements of plasma levels of sedative agent were made. In addition, though Propofol sedation was continuously maintained by intravenous drip, Nembutal sedation was achieved by single oral dose given only at the beginning of the clinical procedure. Thus, due to partial washout, the level of sedation under Nembutal may not have been the same as that under Propofol on average by the end of the procedure when the fMRI acquisition took place. Our study did not include a control group comprised of unsedated infants by which to isolate the specific impact of sedation on activation. The Radiology Department of our hospital does not typically perform MRI in children under 5 years old without sedation. Nevertheless, we can confirm that the activations observed under sedation align with previous results from our laboratory for story listening in older children scanned while awake (41). Substantiation of the offered interpretation of results requires information regarding connectivity, particularly between the fronto-parietal and sensory networks. Future work comparing measures of directed influence, expressed as effective connectivity(42), between these networks for Nembutal and Propofol protocols would be paramount. Finally, the relatively small number of subjects considered in this study hampered sensitivity to differences between the two sedative protocols.

In conclusion, clinical protocols using Nembutal and Propofol to sedate children for MRI procedures, differ in their effect on activation patterns elicited by passively listening to stories. Temporally-resolved assessment of response reveals distinct distribution of activity between an introspective/integrating fronto-parietal network and a lower-level sensory processing network centered on auditory cortex. These differences could influence the methods of image analysis as well as the interpretation of fMRI outcomes in children under sedation when using these protocols. They alert that the clinical target of an fMRI exam should be considered when choosing a sedation protocol. For fMRI probing language under sedation, a Nembutal protocol allows robust activation of auditory function, but induces little in higher-order parietal regions. A Propofol protocol has the disadvantage of suppressing activation overall but with relatively better engagement of activity in higher-order cortices. The results provide impetus for more extensive studies including a focus on effective connectivity with a larger subject base and a more comprehensive set of sedation methods to compare.

Acknowledgments

Grant Support: NIH (R01-DC07186 and R01-HD38578, PI: S. K. Holland)

References

1. Ogawa S, Lee TM, Kay AR, Tank DW. Brain magnetic resonance imaging with contrast dependent on blood oxygenation. Proc Natl Acad Sci U S A. 1990; 87(24):9868–9872. [PubMed: 2124706]
2. Logothetis NK, Wandell BA. Interpreting the BOLD signal. Annu Rev Physiol. 2004; 66:735–769. [PubMed: 14977420]
3. Vannest J, Karunanayaka PR, Schmithorst VJ, Szaflarski JP, Holland SK. Language Networks in Children: Evidence from Functional MRI Studies. Am J Roentgenol. 2009; 192(5):1190–1196. [PubMed: 19380541]
4. Wilke M, Holland SK, Myseros JS, Schmithorst VJ, Ball WS Jr. Functional magnetic resonance imaging in pediatrics. Neuropediatrics. 2003; 34(5):225–233. [PubMed: 14598227]
5. Zur KB, Holland SK, Yuan W, Choo DI. Functional magnetic resonance imaging: contemporary and future use. Curr Opin Otolaryngol Head Neck Surg. 2004; 12(5):374–377. [PubMed: 15377946]
6. Szaflarski JP, Holland SK, Jacola LM, Lindsell C, Privitera MD, Szaflarski M. Comprehensive presurgical functional MRI language evaluation in adult patients with epilepsy. Epilepsy Behav. 2008; 12(1):74–83. [PubMed: 17964221]
7. Tieleman A, Deblaere K, Van Roost D, Van Damme O, Achten E. Preoperative fMRI in tumour surgery. Eur Radiol. 2009; 19(10):2523–2534. [PubMed: 19430795]
8. Redcay, E. Volume PhD. San Diego: University of California San Diego; 2008. FMRI during natural sleep: A novel method to elucidate functional brain organization in typical development and autism; p. 178
9. Pershad J, Wan J, Anghelescu DL. Comparison of propofol with pentobarbital/midazolam/fentanyl sedation for magnetic resonance imaging of the brain in children. Pediatrics. 2007; 120(3):e629–636. [PubMed: 17698968]
10. Leach JL, Holland SK. Functional MRI in children: clinical and research applications. Pediatr Radiol. 2010; 40(1):31–49. [PubMed: 19937236]
11. Alkire MT, Hudetz AG, Tononi G. Consciousness and anesthesia. Science. 2008; 322(5903):876–880. [PubMed: 18988836]
12. Treisman A. Solutions to the binding problem: progress through controversy and convergence. Neuron. 1999; 24(1):105–110. 111–125. [PubMed: 10677031]
13. Greicius MD, Krasnow B, Reiss AL, Menon V. Functional connectivity in the resting brain: a network analysis of the default mode hypothesis. Proc Natl Acad Sci U S A. 2003; 100(1):253–258. [PubMed: 12506194]
14. Mashour GA. Integrating the science of consciousness and anesthesia. Anesth Analg. 2006; 103(4):975–982. [PubMed: 17000815]
15. Sakabe, Matsumoto. Effects of anesthetic agents and other drugs on cerebral blood flow, metabolism, and intracranial pressure. In: Cottrell, Young, editor. Cottrell and Young's Neuroanesthesia. 5. Mosby: Elsevier; 2010.
16. Patel AM, Cahill LD, Ret J, Schmithorst V, Choo D, Holland S. Functional magnetic resonance imaging of hearing-impaired children under sedation before cochlear implantation. Arch Otolaryngol Head Neck Surg. 2007; 133(7):677–683. [PubMed: 17638781]
17. Humphries C, Binder JR, Medler DA, Liebenthal E. Time course of semantic processes during sentence comprehension: an fMRI study. Neuroimage. 2007; 36(3):924–932. [PubMed: 17500009]
18. Karunanayaka PR, Holland SK, Schmithorst VJ, et al. Age-related connectivity changes in fMRI data from children listening to stories. Neuroimage. 2007; 34(1):349–360. [PubMed: 17064940]
19. Schmithorst VJ, Holland SK. Event-related fMRI technique for auditory processing with hemodynamics unrelated to acoustic gradient noise. Magn Reson Med. 2004; 51(2):399–402. [PubMed: 14755667]
20. Mugler JP 3rd, Brookeman JR. Three-dimensional magnetization-prepared rapid gradient-echo imaging (3D MP RAGE). Magn Reson Med. 1990; 15(1):152–157. [PubMed: 2374495]
21. Schmithorst VJ, Dardzinski BJ, Holland SK. Simultaneous correction of ghost and geometric distortion artifacts in EPI using a multiecho reference scan. IEEE Trans Med Imaging. 2001; 20(6):535–539. [PubMed: 11437113]

22. Altaye M, Holland SK, Wilke M, Gaser C. Infant brain probability templates for MRI segmentation and normalization. Neuroimage. 2008; 43(4):721–730. [PubMed: 18761410]
23. Friston KJ, Holmes AP, Price CJ, Buchel C, Worsley KJ. Multisubject fMRI studies and conjunction analyses. Neuroimage. 1999; 10(4):385–396. [PubMed: 10493897]
24. Turken AU, Dronkers NF. The neural architecture of the language comprehension network: converging evidence from lesion and connectivity analyses. Front Syst Neurosci. 2011; 5:1. [PubMed: 21347218]
25. Yarkoni T, Speer NK, Zacks JM. Neural substrates of narrative comprehension and memory. Neuroimage. 2008; 41(4):1408–1425. [PubMed: 18499478]
26. Binder JR, Desai RH, Graves WW, Conant LL. Where is the semantic system? A critical review and meta-analysis of 120 functional neuroimaging studies. Cereb Cortex. 2009; 19(12):2767–2796. [PubMed: 19329570]
27. Maldjian JA, Laurienti PJ, Kraft RA, Burdette JH. An automated method for neuroanatomic and cytoarchitectonic atlas-based interrogation of fMRI data sets. Neuroimage. 2003; 19(3):1233–1239. [PubMed: 12880848]
28. Xu J, Kemeny S, Park G, Frattali C, Braun A. Language in context: emergent features of word, sentence, and narrative comprehension. Neuroimage. 2005; 25(3):1002–1015. [PubMed: 15809000]
29. Baars BJ, Franklin S. An architectural model of conscious and unconscious brain functions: Global Workspace Theory and IDA. Neural Netw. 2007; 20(9):955–961. [PubMed: 17998071]
30. Dehaene S, Changeux JP. Experimental and theoretical approaches to conscious processing. Neuron. 2011; 70(2):200–227. [PubMed: 21521609]
31. Dueck MH, Petzke F, Gerbershagen HJ, et al. Propofol attenuates responses of the auditory cortex to acoustic stimulation in a dose-dependent manner: a FMRI study. Acta Anaesthesiol Scand. 2005; 49(6):784–791. [PubMed: 15954960]
32. Fransson P. Spontaneous low-frequency BOLD signal fluctuations: an fMRI investigation of the resting-state default mode of brain function hypothesis. Hum Brain Mapp. 2005; 26(1):15–29. [PubMed: 15852468]
33. Boveroux P, Vanhaudenhuyse A, Bruno MA, et al. Breakdown of within- and between-network resting state functional magnetic resonance imaging connectivity during propofol-induced loss of consciousness. Anesthesiology. 2010; 113(5):1038–1053. [PubMed: 20885292]
34. Schrouff J, Perlbarg V, Boly M, et al. Brain functional integration decreases during propofol-induced loss of consciousness. Neuroimage. 2011; 57(1):198–205. [PubMed: 21524704]
35. Davis MH, Coleman MR, Absalom AR, et al. Dissociating speech perception and comprehension at reduced levels of awareness. Proc Natl Acad Sci U S A. 2007; 104(41):16032–16037. [PubMed: 17938125]
36. Liu X, Lauer KK, Ward BD, Rao SM, Li SJ, Hudetz AG. Propofol disrupts functional interactions between sensory and high-order processing of auditory verbal memory. Hum Brain Mapp. 2011
37. Boly M, Garrido MI, Gosseries O, et al. Preserved feedforward but impaired top-down processes in the vegetative state. Science. 2011; 332(6031):858–862. [PubMed: 21566197]
38. Boly M, Moran R, Murphy M, et al. Connectivity changes underlying spectral EEG changes during propofol-induced loss of consciousness. J Neurosci. 2012; 32(20):7082–7090. [PubMed: 22593076]
39. Ramani R, Qiu M, Constable RT. Sevoflurane 0. 25 MAC preferentially affects higher order association areas: a functional magnetic resonance imaging study in volunteers. Anesth Analg. 2007; 105(3):648–655. [PubMed: 17717218]
40. Martin-Loeches M, Casado P, Hernandez-Tamames JA, Alvarez-Linera J. Brain activation in discourse comprehension: a 3t fMRI study. Neuroimage. 2008; 41(2):614–622. [PubMed: 18394923]
41. Vannest JJ, Karunanayaka PR, Altaye M, et al. Comparison of fMRI data from passive listening and active-response story processing tasks in children. J Magn Reson Imaging. 2009; 29(4):971–976. [PubMed: 19306445]

42. Ferrarelli F, Massimini M, Sarasso S, et al. Breakdown in cortical effective connectivity during midazolam-induced loss of consciousness. Proc Natl Acad Sci U S A. 2010; 107(6):2681–2686. [PubMed: 20133802]

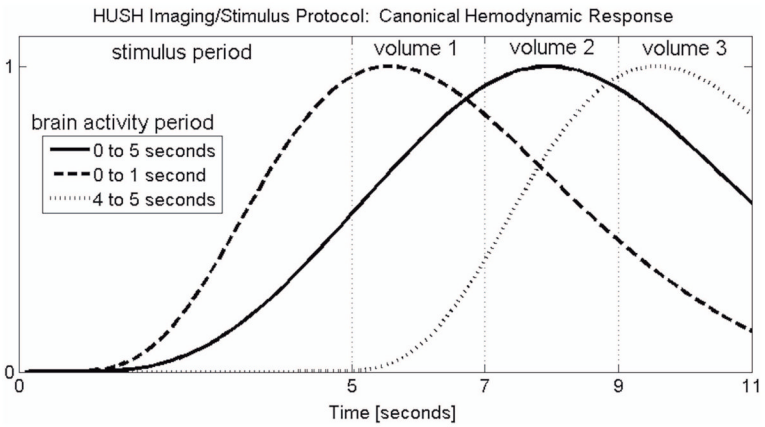

Figure 1.

One epoch of the HUSH protocol showing the 5-second stimulus period and the subsequent three image volumes, each with TR=2s. The solid curve is the canonical hemodynamic response assuming brain activity invoked during the entire stimulus period. The dashed line is the response assuming brain activity only during the first second and the dotted line corresponds to response assuming activity only during the final second of the stimulus period.

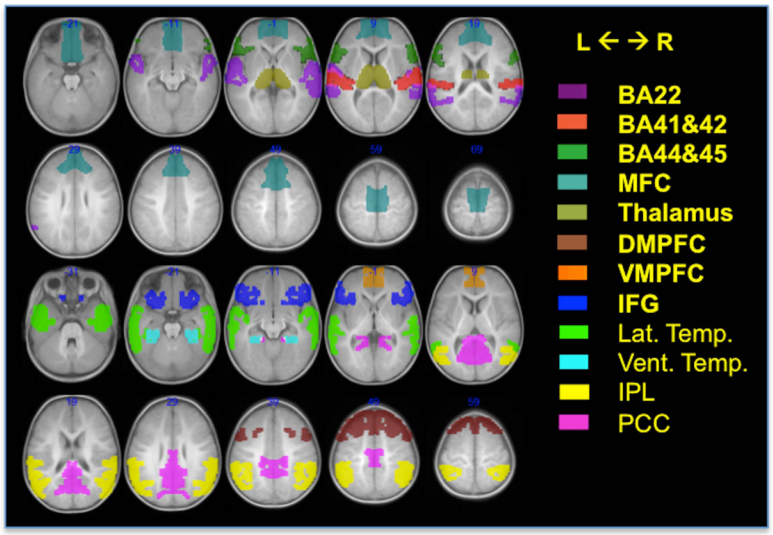

Figure 2.

Anatomical regions of interest. The left and right hemisphere portions of each were considered separately for analysis. BA = Brodmann Area, MFC = medial frontal cortex, DMPFC = dorsal-medial prefrontal cortex, VMPFC = ventral-medial prefrontal cortex, IFG = inferior frontal gyrus, Lat. Temp. = lateral temporal, Vent. Temp. = ventral temporal, IPL = inferior parietal lobule, PCC = posterior cingulate cortex.

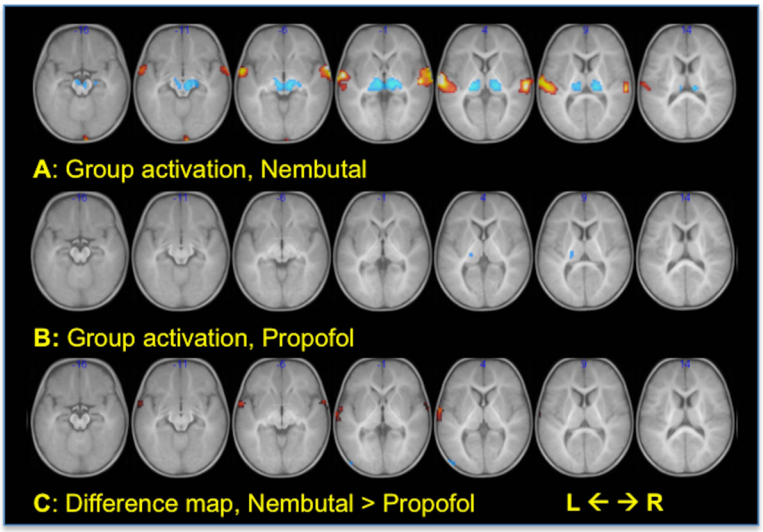

Figure 3.
Group composite parametric maps of mean activation for the contrast between story-listening and silence. For the group maps, A and B, hot/cool colors = activation/deactivation. For the difference map, C, hot colors = Nembutal > Propofol, cool colors = Propofol> Nembutal. For all, $p < 0.005$ uncorrected, cluster threshold = 20 voxels. Numbers indicate MNI z coordinate.

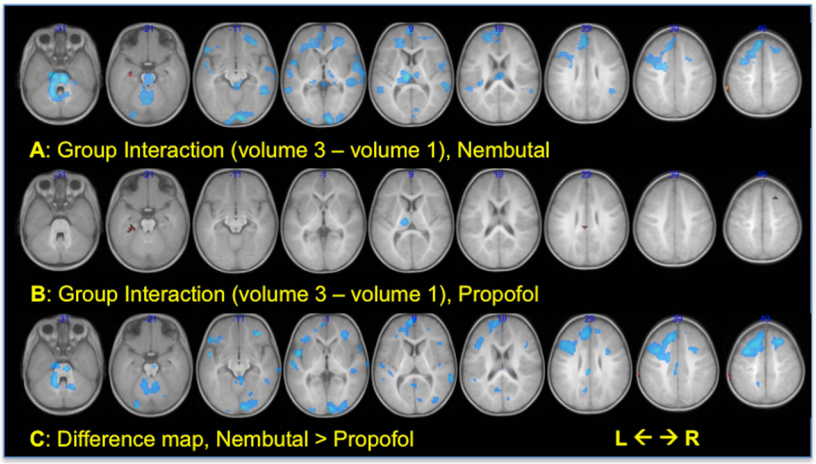

Figure 4.

Group composite parametric maps of the interaction between condition (contrasting story-listening with silence) and time (image volume). For the group maps, A and B, hot colors = volume 3 > volume 1 (positive slope), cool colors = volume 1 > volume 3 (negative slope). For the difference map, C, hot colors = Nembutal slope > Propofol slope, cool colors = Propofol slope > Nembutal slope. For all, $p < 0.005$ uncorrected, cluster threshold = 20 voxels. Numbers indicate MNI z coordinate.

Table 1

Subject backgrounds.

Propofol Group

Age (mos.)	Gender	Race	Dosage	Referral
11	F	Caucasian	Bolus induction with 30+20+20mg Propofol. 200 mcg/kg/min infusion maintenance	
9	F	Caucasian	Induced with sevofluorane 8%, reduced to 4%. 20 mg bolus Propofol, 180 mcg/kg/min increased to 200 mcg/min.	Pierre Robin sequence, continuous vomiting
15	M	Caucasian	Induced with 8% sevofluorane. 200 mcg/kg/min infusion.	h/o repetitive tongue movements. r/o mass.
9	F	Caucasian	Induced with 8% sevofluorane. 200 mcg/kg/min infusion, increased to 225 mcg/kg/min.	seizures
17	F	Caucasian	Induced with 8% sevofluorane. 200 mcg/kg/min infusion, increased to 250 mcg/kg/min.	seizures
9	F	Caucasian	Induced with 8% sevofluorane, two boluses of 10mg Propofol IV followed by 200 mcg/kg/min infusion, added 10mg Propofol bolus. Infusion later increased to 300 mcg/kg/min.	r/o chiasmal lesion
13	F	Caucasian	Induced with 8% sevofluorane, bolus 10 mg Propofol, 200 mcg/kg/min infusion, added bolus 50 mg, increased to 300 mcg/kg/min, then reduced to 250 mcg/kg/min then increased to 295 mcg/kg/min	seizures
11	F	Multiple	Induced with 8% sevofluorane, 20 mg bolus Propofol, 200 mcg/kg/min infusion, then 20mg bolus Propofol	r/o Chiari, feeding disorder
15	F	Caucasian	20 mg bolus Propofol, 250 mcg/kg/min. infusion	retinoblastoma

Nembutal Group

Age (mos.)	M/F	Race	Dosage	Referral
14	F	Caucasian	5.0 mg/kg PO	seizures
17	F	Caucasian	5.0 mg/kg PO	seizures
9	M	Caucasian	5.0 mg/kg PO	h/o motor delay. r/o nystagmus
11	M	Caucasian	5.0 mg/kg PO	History of clonus in lower extremities.
12	F	Caucasian	5.0 mg/kg PO	seizures
16	F	Caucasian	5 mg/kg PO	h/o headaches, r/o mass
13	F	African American	5 mg/kg	r/o mass, nystagmus, spasmus nutans, r/o chiasmal lesion
9	F	Caucasian	5 mg/kg	seizures and left arm weakness.
9	M	Caucasian	5 mg/kg, 40 mg PO	torticollis
15	M	Caucasian	5 mg/kg PO	gross motor delay, macrocephaly
8	F	Other	5 mg/kg PO, then 2 mg bolus/IV	congenital ocular motor apraxia

h/o = ‘history of”, r/o = “rule out”, PO = “by mouth”

Table 2

Mean Response for 3 Image Volumes

		Activation			Deactivation		
Drug	**Contrast**	**Brain Region**	**Peak Voxel Location**	**Cluster p-value**	**Brain Region**	**Peak Voxel Location**	**Cluster p-value**
Nembutal	Stories > Silence	BA22, L	−66, −7, 2	0.004	Thalamus, L	−6, −19, −−2	0.005
		BA22, R	66, −22, 6	0.009	Thalamus, R	12, −22, −2	0.004
		BA41&42, L	−69, −10, 6	0.007			
		BA41&42, R	66, −22, 6	0.023			
		Lateral Temporal, L	−66, −4, −2	0.031			
		Lateral Temporal, R	57, −13, −2	0.049			
	Stories > Tones	---	---	---	Thalamus, R	15, −25, 2	0.050
	Tones > Silence	---	---	---	---	---	---
Propofol	Stories > Silence	---	---	---	---	---	---
	Stories > Tones	---	---	---	---	---	---
	Tones > Silence	---	---	---	IPL, R	30, −40, 54	0.046

Table 3

Condition x Image Volume Interaction

		Negative Slope (Volume 3 < Volume 1)		
Drug	**Contrast**	**Brain Region**	**Peak Voxel Location**	**Cluster p**
Nembutal	Stories > Silence	Thalamus, L	−6, −22, 10	0.004
		Thalamus, R	9, −19, 14	0.026
		DMPFC, L	−6, 38, 50	0.002
		VMPFC, L	−6, 56, 2	0.007
		MFC, L	−6, 56, 2	<0.001
		IFG, L	−54, 26, −10	0.041
		Lateral Temporal, R	45, −31, −2	0.020
		BA22, R	60, 2, 2	0.017
		BA22, R	66, −40, 10	0.018
		Brainstem	−12, −34, −34	<0.001*
		BA18, Occipital, R	6, −97, −6	0.007*
	Stories > Tones	MFC, L	42, 47, −6	0.042
		IPL, L	−48, −64, 28	0.034
		Cerebellum, Vermis	3, −64, −34	0.017*
	Tones > Silence	Thalamus, R	12, −10, 10	0.048
Propofol	Stories > Silence	Thalamus, L	−6, −19, 6	0.021
	Stories > Tones	---	---	---
	Tones > Silence	---	---	---

	Propofol > Nembutal		
Contrast	**Brain Region**	**Peak Voxel Location**	**Cluster p**
Stories > Silence	DMPFC, R	36, 38, −10	0.013
	DMPFC, L	−21, 20, 54	<0.001
	VMPFC, L	−6, 62, 10	0.009
	MFC, L	−6, 62, 10	<0.001
	Brainstem	−15, −34, −34	0.006*
	BA18, Occipital, R	6, −97, −6	0.005*
Stories > Tones	BA18, Occipital, R	30, −85, −10	<0.001*
Tones > Silence			

Table 4

ROI Mean Response All 3 Volumes

		Activation		Deactivation	
Drug	**Contrast**	**Brain Region**	**p-value FDR**	**Brain Region**	**p-value FDR**
Nembutal	Stories > Silence	BA41&42, L	<0.001	Thalamus, L	0.018
		BA22, L	<0.001	Thalamus, R	0.019
		BA22. R	0.017		
	Stories > Tones	---	---	---	---
	Tones > Silence	---	---	VMPFC, R	<0.001
				MFC, R	0.043
Propofol	Stories > Silence	BA41&42, L	<0.001	Thalamus, L	0.005
		BA41&42, R	0.002		
		IPL, L	<0.001		
		IPL, R	0.004		
	Stories > Tones	BA41&42, L	0.037	---	---
		BA41&42, R	0.030		
		IPL, L	0.044		
		IPL, R	0.031		
	Tones > Silence	---	---	---	

Table 5

ROI Condition x Image Volume Interaction

		Positive Slope		Negative Slope	
Drug	**Contrast**	**Brain Region**	**p-value FDR**	**Brain Region**	**p-value FDR**
Nembutal	Stories > Silence	---	---	Thalamus, L	<0.001
				Thalamus, R	0.014
				DMPFC, L	<0.001
				DMPFC, R	0.012
				VMPFC, L	0.012
				VMPFC, R	0.024
				MFC, L	0.001
				MFC, R	0.015
				BA22, L	0.002
				BA22, R	0.002
				BA41&42, L	0.043
				BA41&42, R	0.012
				PCC, L	0.024
				IPL, R	0.012
				BA44&45, L	0.042
	Stories > Tones	---	---	Thalamus, L	0.039
				DMPFC, L	0.024
				DMPFC, R	0.046
				MFC, L	0.023
				BA22, L	0.037
				BA22, R	0.032
				BA41&42, R	0.040
	Tones > Silence	---	---	DMPFC, L	0.044
Propofol	Stories > Silence	BA44&45, R	<0.001	Thalamus, L	<0.001
		IFG, R	0.003	Thalamus, R	0.016
		Ventral Temp., L	0.007		
		DMPFC, L	0.013		

Drug	Contrast	Positive Slope		Negative Slope	
		Brain Region	**p-value FDR**	**Brain Region**	**p-value FDR**
		DMPFC, R	0.018		
		PCC, L	0.014		
		MFC, L	0.016		
		VMPFC, L	0.033		
	Stories > Tones	---	---	---	---
	Tones > Silence	BA41&42, L	0.002	Thalamus, L	0.007
		BA44&45, L	0.010	Thalamus, R	0.013
		BA44&45, R	0.023		
		BA22, L	0.022		
		DMPFC, L	0.022		
		VMPFC, L	0.015		

Table 6

ROI Condition x Image Volume Interaction: Group Differences

	Propofol > Nembutal	
Contrast	**Brain Region**	**p-value FDR**
Stories > Silence	DMPFC, L	<0.001
	DMPFC, R	<0.001
	VMPFC, L	<0.001
	VMPFC, R	0.003
	MFC, L	<0.001
	MFC, R	0.003
	BA22, L	<0.001
	BA22, R	<0.001
	BA41&42, L	0.015
	BA41&42, R	0.016
	PCC, L	<0.001
	PCC, R	0.011
	IPL, L	0.047
	IPL, R	0.014
	BA44&45, L	0.016
	BA44&45, R	0.003
	IFG, L	0.018
	Ventral Temp, L	0.015
Stories > Tones	DMPFC, L	0.005
	IPL, L	0.019
	PCC, L	0.046
	MFC, L	0.016
	MFC, R	0.047
Tones > Silence	BA44&45, L	0.030
	DMPFC, L	0.002
	VMPFC, L	0.004